

Brown coloring electrochromic devices based on NiO–TiO₂ layers

A. Al-Kahlout^a, A. Pawlicka^b, M. Aegerter^{a,*}

^a*Department of Coating Technology, Leibniz Institut für Neue Materialien INM, Im Stadtwald, Gebaeude 2 2, 66123 Saarbruecken, Germany*

^b*Departamento de Físico Química, Instituto de Química de São Carlos, Universidade de São Paulo, C.P. 780, CEP 13560 970, São Carlos SP, Brazil*

Abstract

Brown coloring electrochromic $5 \times 10 \text{ cm}^2$ windows with the configuration K glass/NiO TiO₂/electrolyte/CeO₂ TiO₂/K glass have been prepared and characterized by optoelectrochemical techniques (cyclic voltammetry, chronoamperometry and galvanostatic measurements). The electrochromic layers have been prepared by the sol gel technique. As electrolyte either a 1 M aqueous KOH solution or a newly developed starch based gel impregnated with KOH have been used. The CeO₂ TiO₂ sol gel layers sintered at 550 °C have been previously characterized in 1 M aqueous KOH electrolyte as a function of the thickness up to 2000 cycles and showed a highly reversible behavior without any corrosion effect. The NiO TiO₂ sol gel layers sintered at 300 °C have been extensively characterized in the same electrolyte up to about 7000 cycles. All windows present a deep brown color characteristic of the presence of Ni³⁺ (NiOOH) species, that is fully reversible for several thousands of cycles with a rather fast kinetics (<30 s). The transmittance of the bleached state however slowly decreases with cycling (permanent coloration). The full bleached condition can be nevertheless recovered by applying a negative potential for a long duration. Deeper coloration is usually obtained by cycling the windows galvanostatically with a current density of 20 $\mu\text{A}/\text{cm}^2$. The lifetime of the windows is however limited because of the degradation of the NiO based layers due to the not fully reversible exchange of OH⁻ that turns the layers mechanically fragile and leads eventually to their complete removal from the substrate. Windows working satisfactorily up to 7000 and 17000 cycles have been obtained using aqueous KOH electrolyte and starch KOH gel electrolyte,

respectively. Memory tests showed that the devices bleach at the open circuit potential from $T = 39\%$ (colored state) to about $T = 50\%$ in 60 min.

Keywords: Electrochromic devices; Sol-gel layers; NiO/TiO₂ films; CeO₂/TiO₂ films; Starch based electrolyte; KOH electrolyte

1. Introduction

Electrochromic (EC) materials belong to the family of chromogenics materials and are optically active as their transmittance, absorption and reflectance can be controlled by applying an external field [1]. Most of the research activities in the field of electrochromism have been focused on materials whose optical properties can be modulated in the visible and infrared region [2]. These were driven by the countless proposed applications for their use for large-area glazing in buildings, automobiles, aircrafts, certain types of electronic displays, sunglasses and mirrors. The latter devices are the most successful present application and several millions of them have been produced [3]. Smart windows are able to combine two features that are often thought to be incompatible: (a) energy efficiency with the aim to reduce the cost of air conditioning; and (b) indoor comfort to reduce dazzling and thermal discomfort [4]. They can be built in a form of an electrochemical cell with one or two electrochemically active coatings that change color during a reduction–oxidation process.

Nickel oxide (NiO) is one of such active and low-cost materials. Using highly basic electrolyte (e.g. LiOH and KOH), thin layers change their color anodically from transparent to deep brown and are reversibly bleached when a negative potential is applied [5]. The coloration process has a high coloration efficiency, up to $36 \text{ cm}^2/\text{C}$ [6], a value comparable to that of WO₃, the most studied EC material. This material is therefore useful as a coloring anodic counter electrode to enhance the contrast of EC devices built with a blue coloring cathodic material like WO₃, where natural gray color can be obtained [7–12] or with a gray coloring Nb₂O₅ layers [13]. It could be used also as an active EC layer with a passive counter electrode. It is also worthwhile to remark that NiO can color brown cathodically and bleach anodically when using a LiClO₄-based electrolyte [14,15].

Recently a new sol–gel material (NiO–TiO₂) has been developed by us to get EC coatings with improved EC properties and better adhesion to the substrate when measured in KOH electrolyte. It consists of NiO crystalline nanoparticles (bunsenite structure) imbedded in an amorphous TiO₂ network and the best results have been obtained with a Ni molar concentration of 75% and a sintering between 300 and 350 °C. Such coatings nevertheless degrade after about 7000–10 000 cycles [15,16].

In laminated EC devices as, e.g. those made with sol–gel technologies, the electrolyte has to be preferentially inserted in a liquid state between the EC and the counter electrodes separated by at least 1 mm. Therefore the cost of these polymeric or nanocomposite systems can be rather high (up to 35 €/m^2). Due to the worldwide tendency to use natural and cheap materials that present no side effects on the human health, an attempt to develop a starch-based electrolyte to be used in solid state NiO-based devices is presented here. Starch is found in leucoplasts of tubers, leaves, seeds and other portions of the plant and is composed of two polymers, amylose and amylopectin. Amylopectin is a branched

chained glucose polymer containing both α -1,4-linear and α -1,6-branched linkage, contributing to the viscosity of the starch-based products. Amylose is approximately one-fourth the amylopectin size.

This paper describes first the preparation of the sol-gel coatings as well as the new electrolyte based on starch impregnated with a KOH solution which polymerises at 85 °C and that have been used to build EC devices with the configuration K-glass/NiO-TiO₂/electrolyte/CeO₂-TiO₂/K-glass where K-glass is a glass substrate coated with a transparent conducting SnO₂:F (FTO) layer (Pilkington). The optoelectrochemical properties of the two EC layers tested in 1 M KOH are then presented. Finally the results of two 5 × 10 cm² windows using as electrolyte either an aqueous 1 M KOH solution or the new starch-based gel impregnated with KOH are shown, compared and discussed.

2. Experimental

2.1. NiO TiO₂ layers

Sol-gel NiO-TiO₂ layers have been recently developed and exhibit, when cycled in KOH electrolyte, a fast switching time (< 10 s), a deep reversible brown coloration, a much better stability and a better adhesion to substrates than pure NiO layers [15,16].

An 0.5 M solution was prepared by dissolving 23.32 g of Ni(CH₃COO)₂ · 4H₂O in 150 ml ethanol at room temperature with continuous stirring for 7 h. Then 8.879 g of titanium *n*-propoxide were dissolved in 100 ml of ethanol and added to the Ni solution in a glove box filled with nitrogen (humidity RH ≤ 5%) to obtain sols with Ni/Ti molar concentration of 3/1. The sols were stirred at room temperature for 30 min, and finally filtered using a 0.2 μm Teflon filter.

NiO-TiO₂ layers were deposited by the dip-coating process (withdrawal speed of 3 mm/s, 20 °C, RH = 40%) onto 5 × 10 cm² commercial conducting SnO₂:F-coated glass having a sheet resistance of 17 Ω/□ (K-glass, Pilkington). On the K-glass substrate 1 cm was left free for electrical connection. A heat treatment in air was performed at a rate of 2 K/min up to 300 °C and then the system was left at this temperature for about 30 min. The dip coating and heating processes were repeated twice to obtain double layers. The thickness of the layers, determined by scratching the layer after drying and measuring the step height using a TENCOR P-10 surface profilometer, was 90 nm for 1 layer and 180 nm for two layers. The coatings consist of small 3–8 nm NiO crystalline particles (bunsenite structure) imbedded in an X-ray amorphous TiO₂ network [15,16].

2.2. CeO₂ TiO₂ layers

Sol-gel CeO₂-TiO₂ layers have been first developed in the group of Aegerter [17] and then improved at INM for their use as passive, noncoloring counter electrodes for EC devices [18].

A CeO₂-TiO₂ sol was prepared first by dissolving 24.4254 g Ce(NO₃)₃ · 6H₂O in 125 ml absolute ethanol (0.45 mol/l Ce), and 19.5429 g Ti(i-OPr)₄ in 125 ml of absolute ethanol (0.55 mol/l Ti). The last solution was added to the cerium nitrate ethanolic solution in a glove box under nitrogen atmosphere. This solution was aged at 30 °C during several days under mechanical stirring in a closed glass vessel to prevent the precipitation of the hydrolyzed alkoxide. The CeO₂-TiO₂ layers were deposited on pre-treated K-glass by the

dip-coating technique with a withdrawal rate of 4 mm/s at 20 °C with 38% air humidity. On the K-glass substrate 1 cm was left free for electrical connection. The layers were heated from room temperature up to 550 °C with a heating rate of 2.5 K/min, maintained at 550 °C for 1 h and then cooled down to room temperature. The coatings also consist of small CeO₂ nanoparticles (size ~2–3 nm) imbedded in an X-ray amorphous TiO₂ network. The thickness of the used single layer was about 200 nm.

2.3. KOH-based starch electrolyte

Starch-based electrolyte was first developed in the group of one of the author [19]. For the present study they have been modified by adding small amount of KOH in the following way: 1.8 g of starch (C₆H₁₀O₅)_n was dissolved in 30 ml of bidistilled water at room temperature. The sol temperature was raised gradually to 85 °C with continuous stirring for 3 h. The sol was then left to cool down to 50 °C with stirring. Small amount of KOH was then dissolved in 5 ml bidistilled water and added to the starch sol, 1.5 g of glycerol (C₃H₈O₃) was added and stirred for min, 0.5 g formaldehyde (CH₂O) could be added to increase the cross-linking of the electrolyte. The electrolyte was filled in the devices as soon as it was prepared.

2.4. Device's lamination

The preparation of the EC devices was done by mounting an adhesive spacer tape (1 mm thick) on the four edges of one of the functional coatings (e.g. NiO–TiO₂). Then the other coated substrate (CeO₂–TiO₂) was pressed onto the first one in such a way that the two coatings faced each other inside the assembled window leaving a space of 1 mm between them. A 1 cm wide Cu-conducting tape was glued to the free edge of each substrate for electrical connection, 1 M KOH-starch viscous gel electrolyte was finally injected in the mounted cells and left for 24 h at room temperature to gel before testing the device. For devices made with liquid aqueous KOH electrolyte, the same procedure was adapted but using a 1 M KOH solution.

2.5. Characterization of the layers and devices

Cyclic voltammetry (CV), chronoamperometry (CA) and galvanostatic (CP) measurements have been performed using an EG&G PAR model 273 computer-controlled potentiostat-galvanostat. In situ and ex situ transmittance measurements were recorded using a Cary 5E UV–VIS–NIR spectrophotometer from Varian. Measurements were performed at a wavelength of $\lambda = 550$ nm or in the UV–VIS–NIR spectral range between 300 and 3000 nm.

3. Results and discussion

The devices that have been studied possess an optically active NiO–TiO₂ layer and an optically passive CeO₂–TiO₂ sol–gel layer in close contact with an electrolyte containing KOH, a highly corrosive base. It was therefore first necessary to obtain information about the behavior of these layers in 1 M KOH liquid electrolyte. The results are given in the next two sections.

3.1. Characterization of $\text{CeO}_2/\text{TiO}_2$ layers in KOH

CV recordings were performed in order to obtain their electrochemical fingerprints (Fig. 1). The potential in each measurement was swept from -1.2 to $+0.7$ V vs. SCE. A well-defined anodic peak occurs at -0.238 V while the cathodic peak occurs at -0.63 V. The stability of the layers was checked by cycling up to 2000 cycles. A stable response was achieved after 50 cycles where no change in peak current density was noticed. The cathodic and anodic charges are almost the same indicating that the process is highly reversible and that no Faradic process occurs in parallel to the EC process.

The dependence of the CV response on the film thickness is depicted in Fig. 2. The current density increases by increasing the thickness up to 240 nm. Increasing the layer thickness also shifts the anodic peak slightly to more positive potential values while the

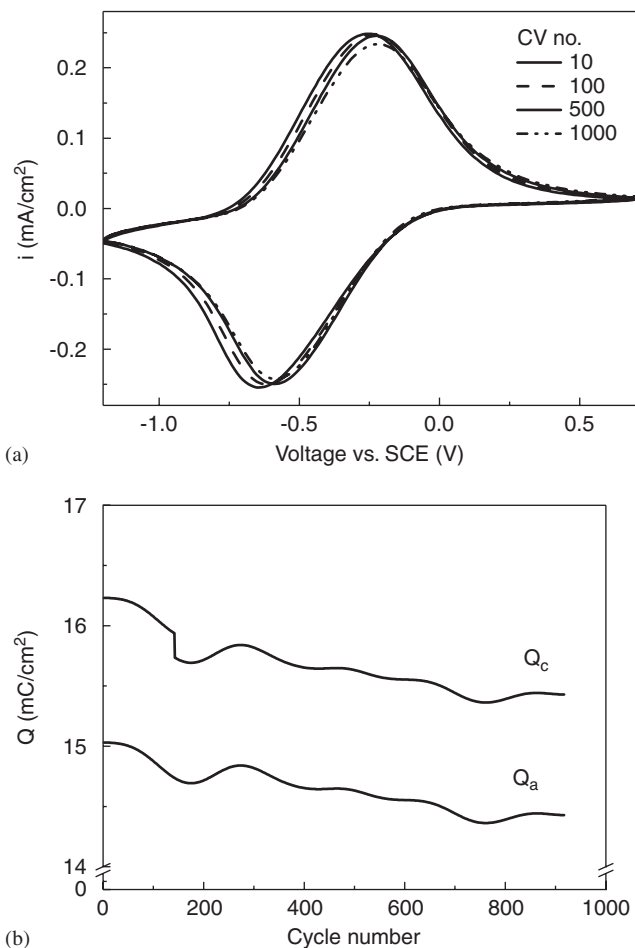


Fig. 1. (a) Typical CV voltammograms up to 1000 cycles for a 200 nm thick single $\text{CeO}_2/\text{TiO}_2$ layer heated at 550°C , potential range -1.2 to 0.7 V vs. SCE, scan rate 10 mV/s in 1 M KOH. (b) Calculated charge density in the anodic (Q_a) and cathodic (Q_c) range.

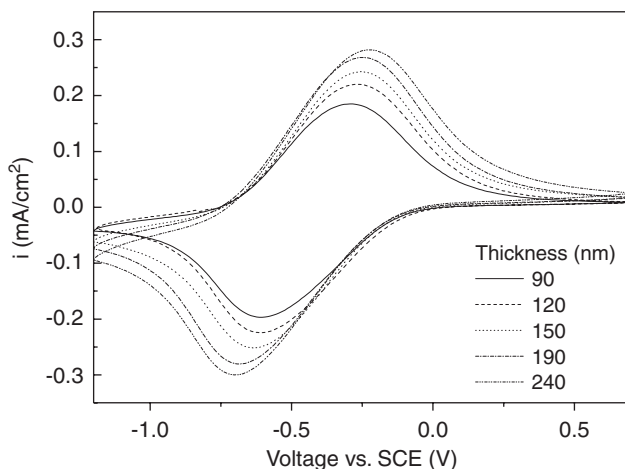


Fig. 2. 100th CV voltammogram (-1.2 , $+0.7$ V vs. SCE, scan rate 10 mV/s) in 1 M KOH of single $\text{CeO}_2/\text{TiO}_2$ layer of different thicknesses heated at 550 °C.

cathodic peak shifts to more negative potentials. The charge density Q_a increases with the thickness from 12 mC/cm² for a 90 nm thick layer to 19 mC/cm² for a 240 nm thick one.

For a redox reaction to be reversible, the concentrations of the oxidized and reduced species at the electrode surface must be maintained at the values required by the Nernst equation. In practical terms, a redox reaction is reversible if the rate of electron transfer is fast relative to the scan rate and if the oxidized and reduced species are stable on the experimental time scale (i.e. they do not undergo any significant chemical reactions [20]). The theoretical peak potential difference for a reversible system should be about 60 – 70 mV (usually the obtained values are about 58 – 59 mV, depending on the temperature and the switching potential). The peak currents should be also equal and the peak potential difference should not change with the scan rate. The results presented in Fig. 3 indicate that these requirements are fulfilled up to about a scan rate of 10 mV/s as the anodic and cathodic peak positions and separations remain *almost* constant indicating a reversible redox reaction.

The current is directly proportional to the rate of electrolysis at the electrode surface that occurs in response to a change in potential in order to maintain the surface concentration of the oxidized and reduced species at the values required by the Nernst equation. Therefore, the faster the rate of change of potential (i.e. the scan rate) is, the faster the rate of electrolysis and hence the larger the currents are. Fig. 4 shows that the anodic current density is proportional to $\nu^{1/2}$ for scan rate ≤ 10 mV/s, indicating a diffusion-controlled process. The determination of the current peaks should be measured from a baseline that is moved to a value that can be predicted only from the decaying portion of the forward peak, a procedure that is unsafe for higher scan rates. No results are therefore shown.

Single 200 nm thick $\text{CeO}_2/\text{TiO}_2$ layers sintered at 550 °C have been also tested in other OH^- -based aqueous electrolytes, namely $\text{C}_{16}\text{H}_{36}\text{NOH}$ and LiOH , both having a pH value of 13 . The layers show basically the same voltammogram characteristics and the same charge capacities. It is therefore concluded that OH^- ions are the species which are

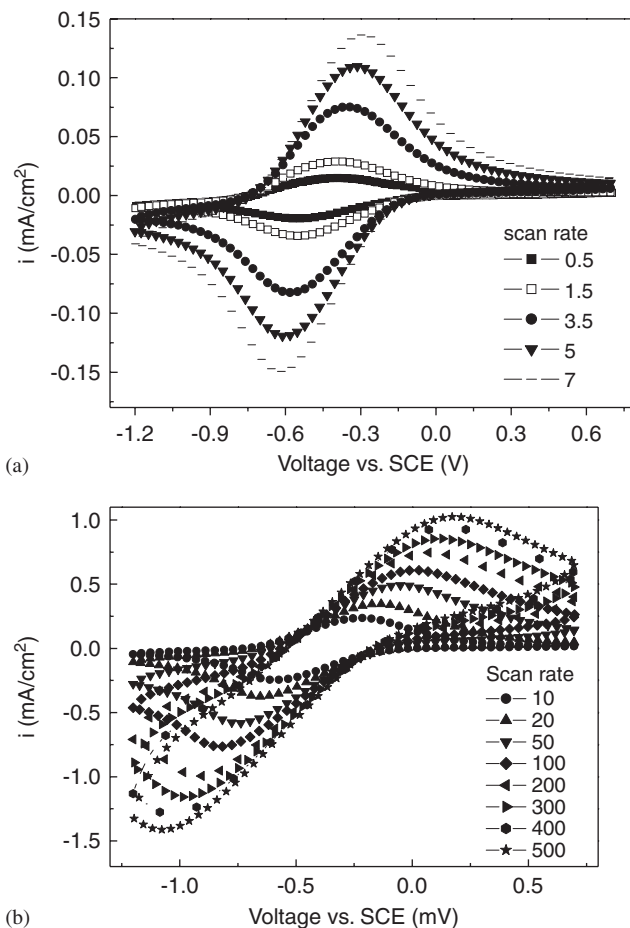


Fig. 3. CV voltammograms (-1.2, +0.7V) of a 170 nm thick single CeO₂/TiO₂ tested in 1 M KOH at different scan rates (a) <math>< 7 \text{ mV/s}</math> and (b) $> 10 \text{ mV/s}$.

responsible for the observed electrochemical activity of the layer in XOH-based aqueous solutions in the potential range -1.2 to +0.7 V vs. SCE.

3.2. Characterization of NiO/TiO₂ layers in KOH

An extensive paper on the properties of NiO-TiO₂ sol-gel layer will appear in Ref. [16], so that only a brief summary is given below.

Pure NiO layers cycled in KOH electrolyte exhibit poor adhesion on FTO/glass substrates and get a rather high permanent brown coloration after already 50 voltammetric cycles. However the adhesion is clearly improved with mixed NiO-TiO₂ layers and the transmittance in the bleached state remains high and constant up to more than 400 cycles. However the change in the absorbance and the charge exchanged decrease continuously on increasing the Ti content. A good compromise was found using Ni molar concentration of

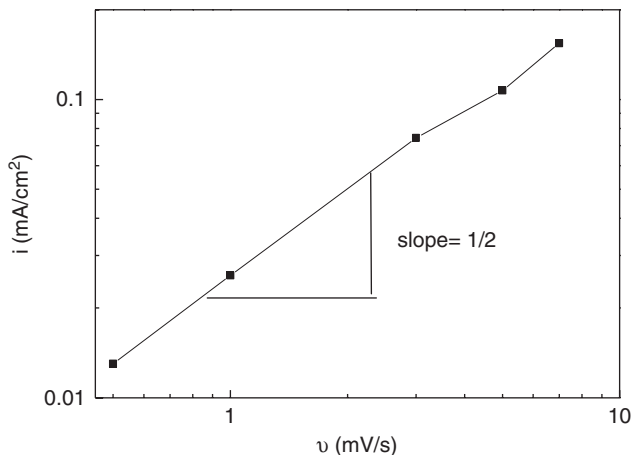


Fig. 4. Log log plot of the anodic peak current density of a 170 nm thick single $\text{CeO}_2/\text{TiO}_2$ tested in 1 M KOH measured during CV (1.2, +0.7 V) versus the corresponding scan rate (up to 10 mV/s).

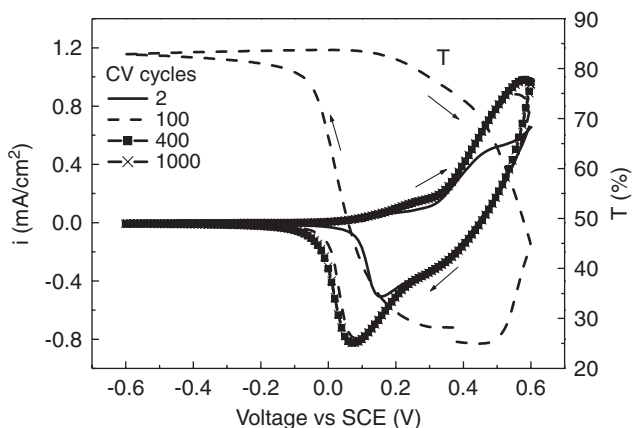


Fig. 5. Typical CV cycles up to 1000 cycles for a 160 nm thick double NiO/TiO_2 layer (Ni concentration of 75 mol%) heated at 300 °C, potential range -0.6 to 0.6 V vs. SCE, scan rate 10 mV/s in 1 M KOH. The dotted line is the variation of the transmittance T measured during the 100th cycle at $\lambda = 550$ nm.

75% and a sintering between 300 and 350 °C [15,16]. These are the layers that have been used to mount and test EC windows.

When cycled between -0.6 and +0.6 V vs. SCE the layers show a deep reversible brown coloration with a transmittance change measured at 550 nm between $T_{\text{bleached}} = 85\%$ and $T_{\text{colored}} = 25\%$ and a fast switching time (< 10 s). Typical CV cycles and transmittance change at 550 nm simultaneously recorded are shown in Fig. 5. By extending the potential range to +1 V, the layers show a darker brown color and a higher absorbance ($\Delta\text{OD}_{550} = 0.8$) with a high coloration efficiency peaking to a value of $52 \text{ cm}^2/\text{C}$ at 400 nm. Typical spectra are shown in Fig. 6.

The EC process exhibits an activation period which may last to about 1000 cycles (depending on the potential range and the thickness of the layer) where the absorbance of

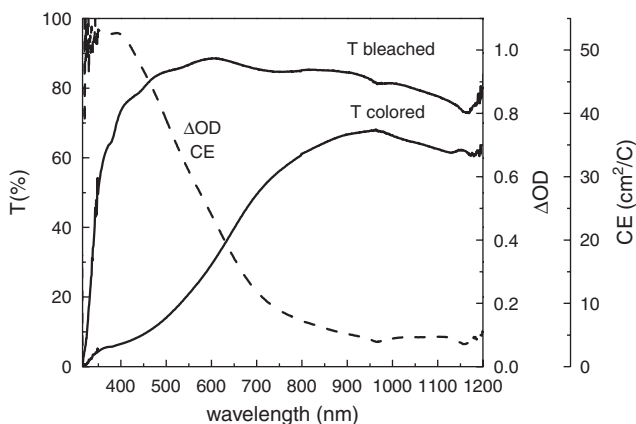


Fig. 6. Optical transmission spectra of a 160 nm thick NiO₂/TiO₂ double layer heated at 300 °C measured in the colored and bleached states during the 50th CV cycle. The layer was bleached and colored by polarizing it for 20 s at -0.6 V and +1 V, respectively. ΔOD and the coloration efficiency are also shown.

the layer increases. It is followed by a degradation period in which a passive, irreversibly colored and fragile layer is built at the electrolyte/layer interface that slowly decreases the change of the absorbance, the value of the transmittance in the bleached state (permanent coloration), the amount of charge exchanged and that drastically increases the fragility of the layers. Nevertheless about 10 000 cycles can be performed before a complete removing of the layer [15,16]. Electrochemical quartz microbalance experiments essentially confirm that the coloration/bleaching process in the activation period is due to the insertion/deinsertion of OH⁻ [15,21].

3.3. EC windows

3.3.1. Windows built with a liquid KOH electrolyte

Windows of area $5 \times 10 \text{ cm}^2$ with the configuration glass/FTO/NiO-TiO₂/1 M liquid KOH/CeO₂-TiO₂/FTO/glass have been laminated following the procedure described in Section 2.4 using either single or double NiO-TiO₂ layers. The windows have been tested in the potential range -1 to +1.2 V.

Fig. 7 shows typical voltammograms of windows made with single and double layers of NiO-TiO₂ layers, measured during the 1000th cycle. They have practically the same shape except a small shift in the anodic and cathodic peak positions. No difference is noticed in the current density of the two windows.

After a few initial cycles, windows made with a *single* NiO-TiO₂ layer present quite interesting optical properties up to 1000 cycles with fast transmittance change from about 60% down to 30% and optical density change around 0.3 (Fig. 8). Then they degrade fast due especially to a continuous increase of the permanent coloration of the bleached state (Fig. 8(a)). After 4000 cycles a corrosion starts to appear at the edge of the windows.

However the use of a *double* layer improves especially the cycling stability and the transmittance of the window in the bleached state that decreases only slightly by cycling from $T = 70\%$ (initial cycles) down to $T = 60\%$ after 7000 CA cycles. Therefore the

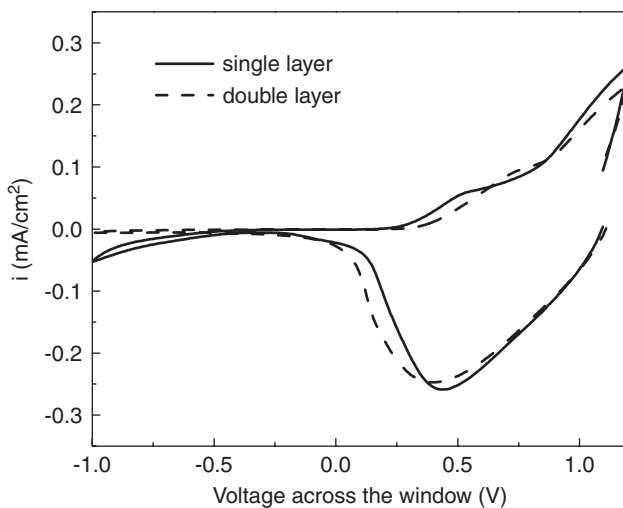


Fig. 7. 1000th CV voltammograms of windows with the configuration K glass/NiO TiO₂/KOH/CeO₂ TiO₂/K glass with single (—) and double (---) NiO TiO₂ layers.

transmittance of the device in the bleached state remains largely unaltered, contrary to the behavior observed with a single layer (Fig. 8(a)). However the transmittance of the colored state is somewhat higher (30% after 7000 cycles). The change of the optical density at 550 nm is consequently different and the device still works very well after 7000 cycles (Fig. 8(b)). Unfortunately by further cycling, degradation starts to occur at the edges of the devices.

It is also interesting to note that practically the same ΔT and ΔOD behavior is observed if one scales down the ordinate of the results obtained using the double layer by a factor seven. The results are therefore fully compatible with the optoelectrochemical properties of such layers summarized in Section 3.2.

By leaving the window built with a double NiO–TiO₂ at the negative potential (–1 V) for different time periods (measurement carried out after cycling the window for 7000 cycles) it was found that the device could be effectively bleached practically to the same initial value after applying the potential for 90 min (Fig. 9). However when the window is cycled again between –1 and 1.2 V (1 min) it could only be bleached to the level it reached before ($T = 59\%$). This means that there are different coloring sites (with two different kinetics) one needed much more energy to be bleached. The β -Ni(OH)₂ are probably the initial sites in the bleached state leading after OH[–] insertion to hydrated NiOOH sites responsible for the coloration and that are slowly transformed by cycling into α -Ni(OH)₂ and γ -NiOOH ones respectively [15].

The transmittance spectra of a window in the bleached and colored states are shown in Fig. 10 with the corresponding ΔOD . The main transmittance change occurs in the visible and the near infrared region with a maximum of ΔOD at 432 nm and the color of the window is brown. The values are somewhat smaller than those obtained by measuring the NiO–TiO₂ layer alone in the same electrolyte (Fig. 6). By cycling the windows with an extended potential range from –1 to +1.9 V, no improvement of the optical properties (e.g. the contrast) has been obtained. On the contrary the use of a higher positive potential

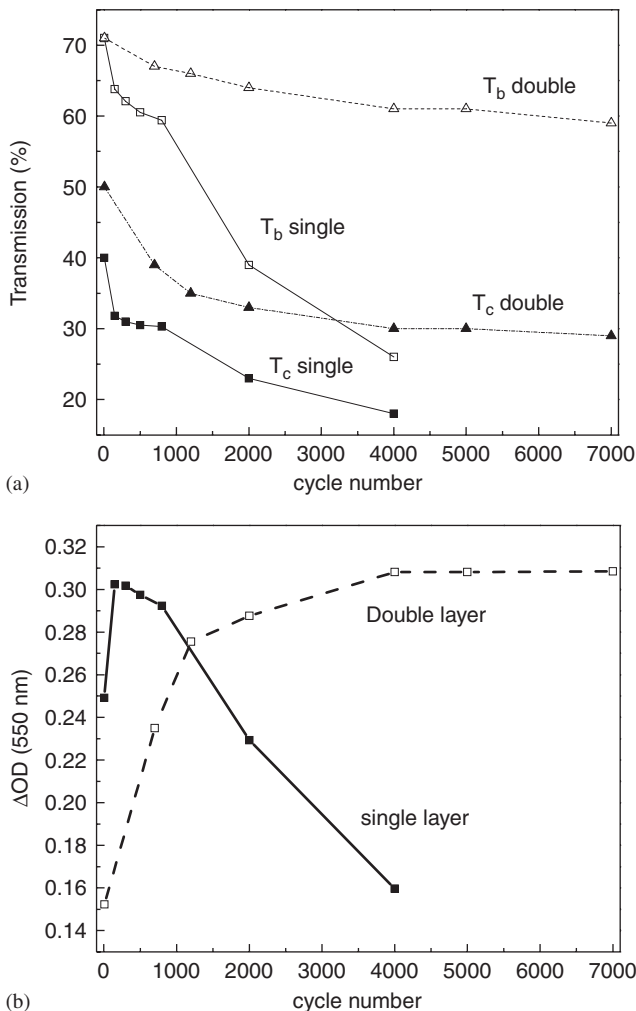


Fig. 8. (a) Transmission of the bleached and coloured states at $\lambda = 550$ nm of an EC device glass/FTO/NiO TiO₂/1 M liquid KOH/CeO₂ TiO₂/FTO/glass mounted with a single and a double NiO TiO₂ layer, during CA cycles (−1 V, +1.2 V, 1 min). (b) Corresponding change in optical density.

led to a faster degradation observed as small but visible areas of the NiO–TiO₂ layer starting to dissolve into the electrolyte.

The long-time stability of the devices based on NiO–TiO₂ double layers is not high (almost 7000 cycles) as layers then degrade when cycled in KOH electrolyte. It is known from the literature that thin layers of dielectric oxides may be used as anticorrosion layers. Following these ideas thin layers of ZrO₂, TiO₂, Al₂O₅ and CeO₂–TiO₂ (all 20–25 nm thick) have been deposited on top of 300 °C sintered NiO–TiO₂ layer to improve the corrosion resistance in KOH electrolyte and therefore the cycling stability. These protective layers have been deposited by dip coating at a very small drawing speed (0.5 mm/s) and then sintered at 300 °C. It was not possible to use higher temperature

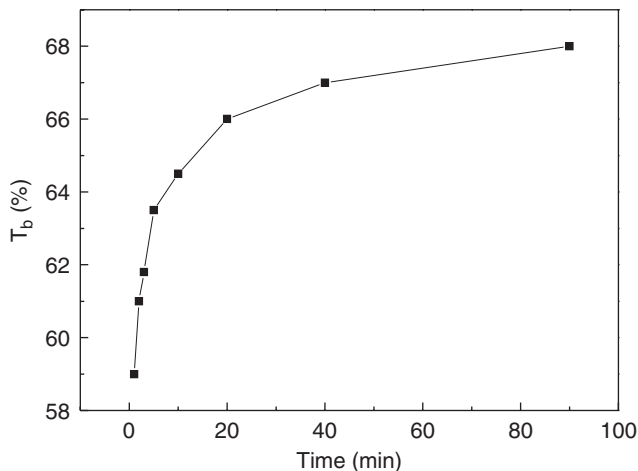


Fig. 9. Transmittance measured at 550 nm of the bleached state reached by polarizing the window at the negative potential (-1 V) for different time periods.

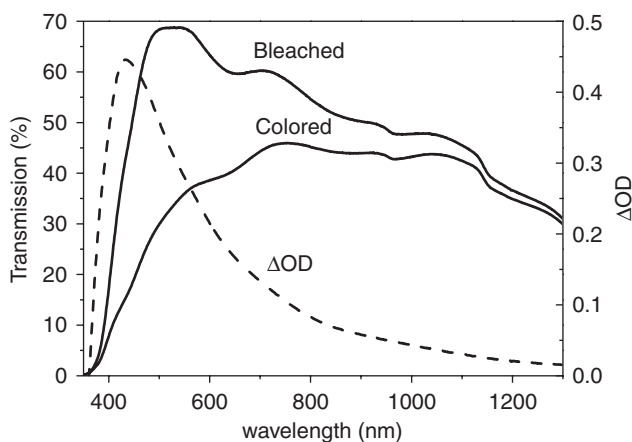


Fig. 10. Transmittance spectra of the bleached and colored states measured during the 1000th cycle of an EC device glass/FTO/NiO-TiO₂/1 M liquid KOH/CeO₂-TiO₂/FTO/glass mounted with a double NiO-TiO₂ layer 160 nm thick. The device was bleached and colored by polarizing it for 1 min at -1 V and $+1.2$ V, respectively. The corresponding ΔOD is also shown.

(> 500 °C) in order to get crystallized dielectric thin films as recommended for anti-corrosion coatings since the high temperature results in poor EC response of NiO-TiO₂ [15]. Fig. 11 shows the CV voltammograms of devices assembled using such NiO-TiO₂ protected layers. The voltammograms keep the same shape with comparable anodic and cathodic current peak densities. Only when ZrO₂ was used, a shift to lower positive potential is noticed with a clear decrease in the current density. The change in optical density of devices built using unprotected and protected *single* NiO-TiO₂ has almost the same behavior. It increases in the beginning (i.e. during activation period) then starts to decrease. The use of protected layers nevertheless improves the long-time stability of the

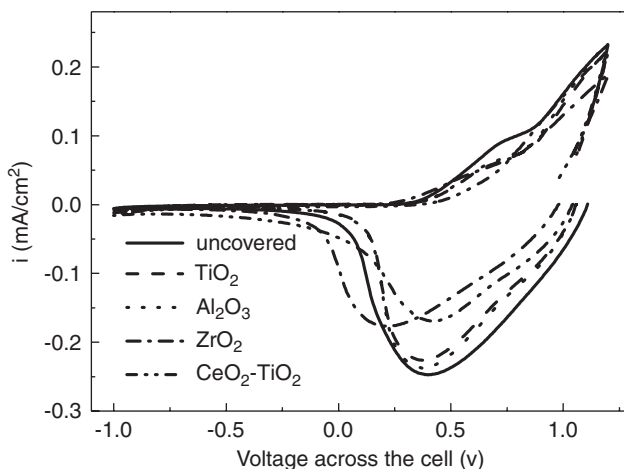


Fig. 11. 1000th CV voltammogram (-1 to +1.2V), scan rate of 10 mV/s of windows with the configuration K glass/protected NiO TiO₂/KOH/CeO₂ TiO₂/K glass.

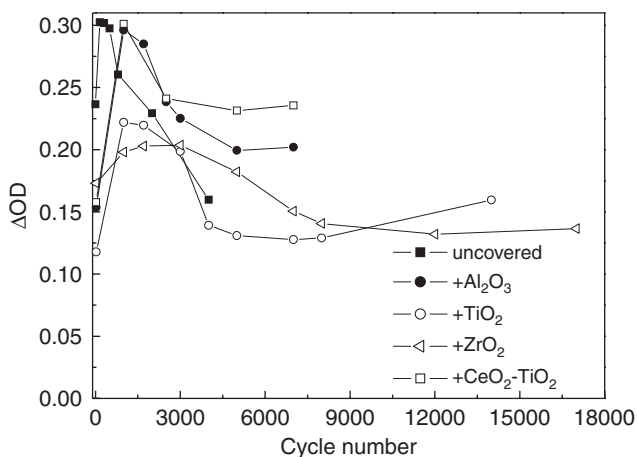


Fig. 12. Change in optical density with the CA cycle number (-1, +1.2V/1 min) of windows with the configuration K glass/protected NiO TiO₂/KOH/CeO₂ TiO₂/K glass.

devices (up to 13 000 cycles (Al₂O₃) and 18 000 cycles with (ZrO₂) but the values of ΔOD are smaller (Fig. 12). Tests are underway using *double* NiO–TiO₂ layers covered with these dielectric corrosion protecting layers for which even longer cyclability is expected.

3.3.2. Windows built with a starch KOH electrolyte

Windows of area $5 \times 10 \text{ cm}^2$ with the configuration K-glass/NiO–TiO₂/starch-KOH/CeO₂–TiO₂/K-glass have been assembled and tested by cyclic voltammetry in the potential range of -0.7 to 1.9 V up to 1700 cycles at a scan rate of 10 mV/s. A *double* NiO–TiO₂ has been used. Fig. 13 shows the first two voltammograms. The same features seen with the window made with liquid 1 M KOH electrolyte are observed. The first cycle presents two anodic peaks, the first one is weak and occurs around 0.8 V while the other is stronger and

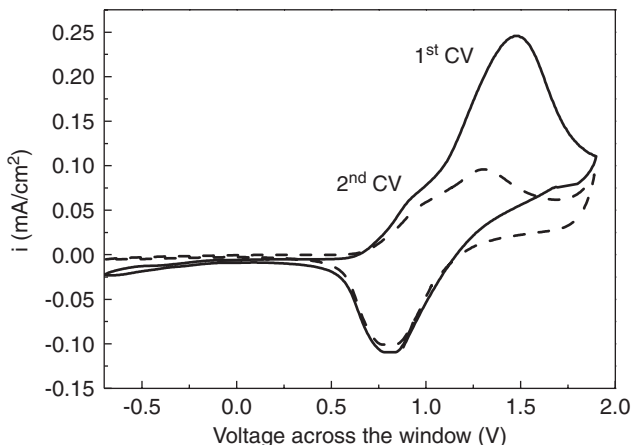


Fig. 13. 1st and 2nd CV voltammograms (0.6 to 0.6 V vs. SCE, scan rate 10 mV/s) of an EC device with the configuration glass/FTO/NiO TiO₂/starch(KOH)/CeO₂ TiO₂/FTO/glass mounted with a double NiO TiO₂ layer 160 nm thick.

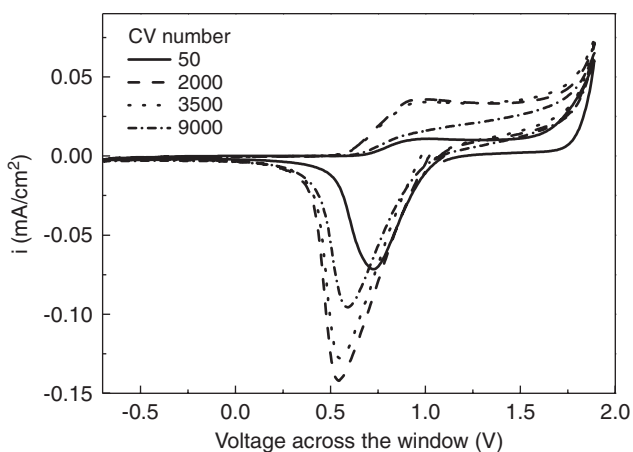


Fig. 14. CV voltammograms (0.6 to 0.6 V vs. SCE, scan rate 10 mV/s) up to 9000 cycles of an EC device with the configuration glass/FTO/NiO TiO₂/starch(KOH)/CeO₂ TiO₂/FTO/glass mounted with a double NiO TiO₂ layer 160 nm thick.

occurs around 1.4 V and is almost completed at +1.9 V. During the second cycle the second anodic peak at 1.4 V practically disappears. Only the first peak at 0.8 V remains so that the anodic current density is strongly reduced. In the cathodic range only one well-defined peak can be observed in the range of 0.7 V that practically does not change.

By further cycling the current density of the anodic peak continues to decrease up to the 50th cycle but then both cathodic and anodic peaks increase continuously up to 2000 cycles and then start to decrease again (Fig. 14). The shape of the voltammograms remains in all cases the same with however a slight shift of the cathodic peak to lower positive potential values (till 2000 cycles) and then to more positive values. Although an increase of the

current density as a function of the cycles was also observed for NiO–TiO₂ layers tested in KOH electrolyte and related to an activation period [15,16] as well as for Ni₂O₃ films [22] and NiO films [23], the drastic change observed in the anodic voltammogram shapes of the present EC device can only be due to some reactions that have occurred with the starch-based electrolyte. They are presently not understood.

Fig. 15 represents the transmittance of the brown coloring window measured at 550 nm in the colored and bleached states as a function of the CA cycle number. As expected from the behavior of the voltammograms, the window shows initially a high transmittance change from around 70% in the bleached state down to 25% in the colored state. This large difference ($\Delta T = 45\%$) decreases however abruptly during the first 50 cycles to reach a value of only $\Delta T = 12\%$. Then the transmittance of the bleached state of the device stabilizes at about $T = 60\%$ followed by a small decrease down to 55% up to the 17000th cycle. The colored state behavior is more complex. The transmittance abruptly increases during the first 50 cycles, starts to decrease, reaching a value of $T = 32\%$ at 2000 cycles and then increases again slowly to reach a value of $T = 48\%$ after 17000 cycles, the difference between the colored and the bleached states transmittance being only $\Delta T = 6\%$ after 17000 cycles.

The transmittance spectra in the bleached and colored states as well as the absorbance change spectrum (ΔOD) are shown in Fig. 16 for the 2000th cycle (highest contrast). The shape of the spectra is similar to those obtained for the NiO–TiO₂ layer (Fig. 8) or for the windows built with a liquid KOH electrolyte. The absorbance change at 550 nm (ΔOD_{550}) versus the cycle number is shown in Fig. 17 together with that recorded for a window built with KOH electrolyte and switched within the same applied potential (-0.7 to $+1.9$ V). For the window built with starch–KOH electrolyte the value is the highest during the first cycle, $\Delta OD = 0.42$, then it drops to 0.1 after 50 cycles, increases up to 0.27 at the 2000th cycle to finally decrease down to 0.1 at the 9000th cycle. On the other side, for the window made with a *double* NiO–TiO₂ layer and a liquid KOH electrolyte a continuous increase of ΔOD is observed to finally reach a plateau with $\Delta OD_{550} = 0.305$ at the 4000th cycle. This

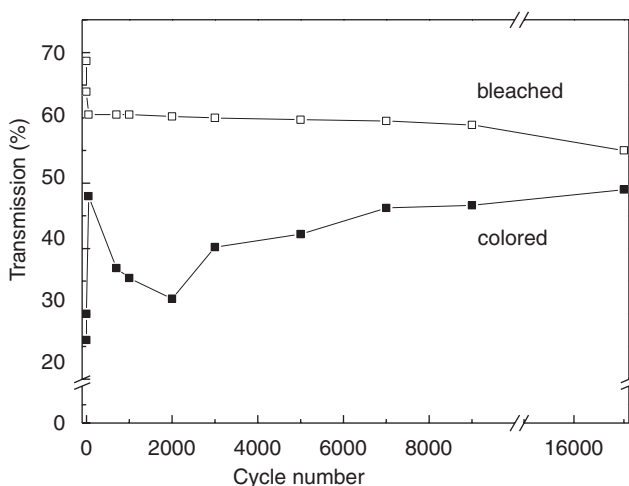


Fig. 15. Transmittance of the bleached and colored states measured at 550 nm versus the CA cycle number (0.7, 1.9V/1 min) of a window with the configuration K glass/NiO TiO₂/starch(KOH)/CeO₂ TiO₂/K glass.

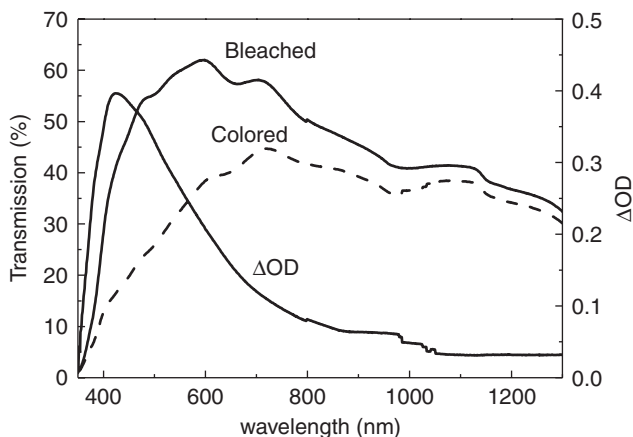


Fig. 16. Transmittance spectrum in the bleached and colored states and absorbance change ΔOD recorded during the 2000th cycle of a window having the configuration glass/FTO/NiO TiO_2 /1 M starch(KOH)/ CeO_2 TiO_2 /FTO/glass obtained by polarization for 1 min at +1.9 and -0.7 V, respectively.

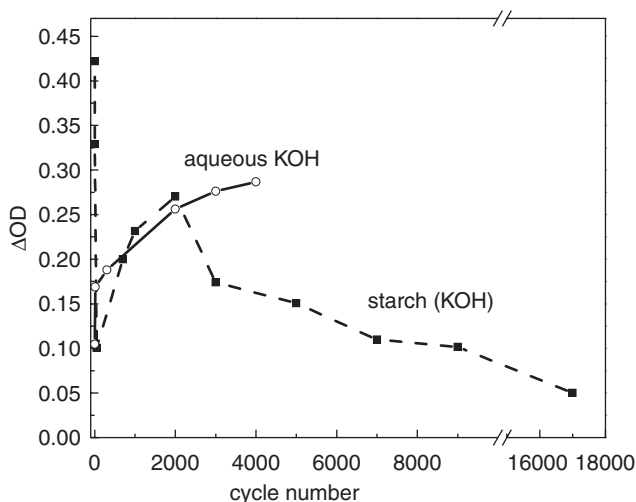


Fig. 17. ΔOD vs. cycle number of a window with the configuration K glass/NiO TiO_2 /starch(KOH)/ CeO_2 TiO_2 /K glass. The solid line is the behavior of a window with the same configuration but filled with the aqueous KOH electrolyte (for comparison).

behavior is similar to that shown in Fig. 8(b) and recorded using a smaller potential range (-1 to +1.2 V) except that ΔOD and the lifetime are smaller. However both windows show a similar behavior between the 50 and the 2000th cycles, but that built with the starch-KOH electrolyte is degraded faster than that built with liquid KOH electrolyte.

Fig. 18 shows the kinetics of the transmittance change of the ECD recorded at the 50, 2000, 3500 and the 9000th cycle. The transmittance changes from about 60% in the bleached state to different values in the colored state depending on the cycle number, confirming the results presented in Fig. 15. The coloration kinetics is rather slow and more than 1 min is necessary to reach a constant coloration. The kinetics of windows made with

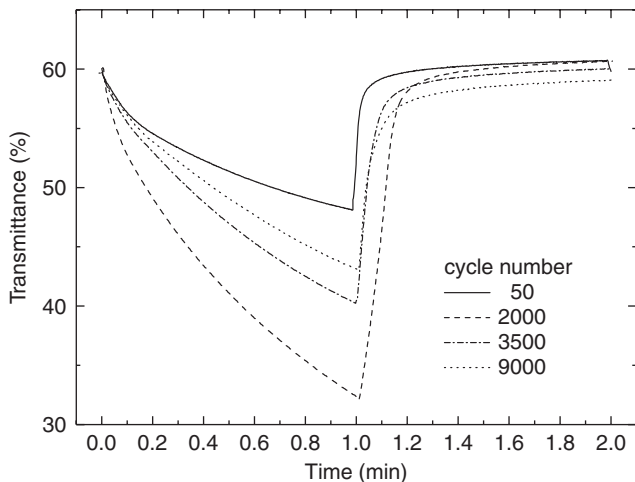


Fig. 18. Time variations of the transmittance measured at 550 nm of windows with the configuration K glass/ NiO TiO₂/starch(KOH)/CeO₂ TiO₂/K glass during CA cycles (0.7 V, 1.9/1 min).

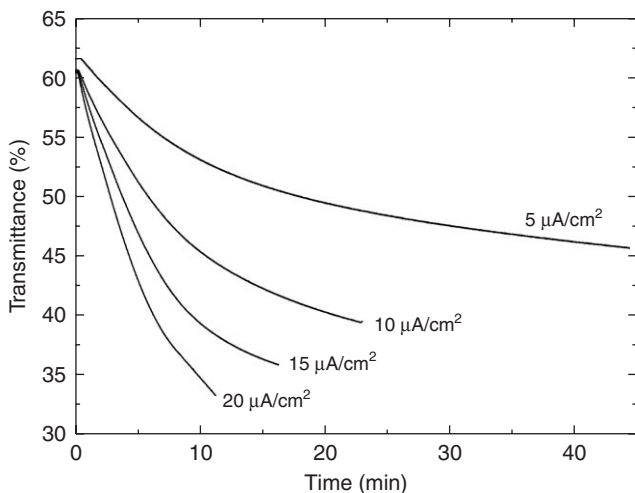


Fig. 19. Evolution of the transmittance of windows with the configuration K glass/NiO TiO₂/starch(KOH)/ CeO₂ TiO₂/K glass during galvanostatic measurements performed using different current densities.

liquid KOH electrolyte is however faster (<30 s) and remains rather constant during cycling [15]. The bleaching kinetics is on the contrary very fast and it takes less than 20 s to bleach completely the window whatever the cycle number is. With an aqueous KOH electrolyte the values are somewhat higher but in the same order of magnitude.

In order to check the possibility to get deeper color of the devices, galvanostatic measurements have been performed after 2000 CV cycles (highest contrast) by applying a current density of 5, 10, 15 and 20 $\mu\text{A}/\text{cm}^2$ and limiting in all cases the total de-inserted charge to 13 mC/cm^2 . Fig. 19 shows that the coloration kinetics get faster and the color

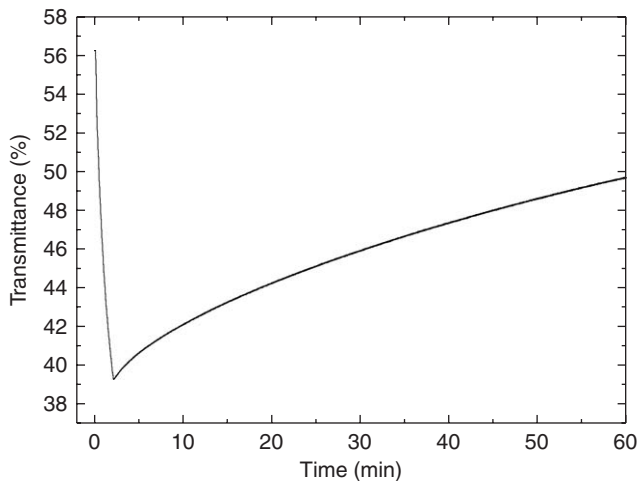


Fig. 20. Evolution of the transmittance of a window with the configuration K glass/NiO TiO₂/starch(KOH)/CeO₂ TiO₂/K glass in open circuit configuration after being colored at +1.9 V for 1 min.

deeper when the current density increases. It is interesting to note that the potential across the window never exceeded a safe level of 2 V in all cases. The transmittance of the window dropped from $T = 63\%$ down to $T = 46\%$ when $+5 \mu\text{A}/\text{cm}^2$ was applied during 44 min and when using $+20 \mu\text{A}/\text{cm}^2$ a value of $T = 33\%$ was reached in 11 min.

The investigated ECDs have been also submitted to a memory test. Fig. 20 shows the result obtained after 3000 CV cycles. The device was colored at +1.9 V for 1 min to reach a transmittance of $T = 39\%$. In open circuit, the device starts to bleach to reach a transmittance value of about $T = 50\%$ after 60 min. This test shows that the investigated ECDs have a rather poor memory.

4. Conclusion

This paper first reported on the opto-electrochemical properties of two sol-gel-processed coatings used in the development of EC devices tested in aqueous KOH electrolyte. One is a new anodic brown coloring NiO-TiO₂ layer and the other is a CeO₂-TiO₂ layer remaining always transparent and that can be used as a passive counter electrode. The first layer exhibits far better EC properties than pure NiO coatings but *single* layers still suffer from corrosion effects after about 4000 cycles and *double* layer after more than 7000 cycles. The second layer, CeO₂-TiO₂, on the contrary shows highly reversible behavior without any corrosion effects.

These layers have been used to build $5 \times 10 \text{ cm}^2$ EC windows with the configuration K-glass/NiO₂-TiO₂/electrolyte/CeO₂-TiO₂/K-glass where the electrolyte was either an aqueous 1 M KOH solution or a newly developed gel electrolyte based on starch impregnated KOH. Some developments have also been done by using NiO-TiO₂ EC layers covered by a thin corrosion-resistant layer such as Al₂O₃, ZrO₂, TiO₂ and CeO₂-TiO₂. All systems have been studied using opto-electrochemical techniques (CV, CA and galvanometry coupled to optical spectroscopy) and show a brown color. The cycling stability was found to be better using the starch-KOH gel electrolyte (typically

17 000 cycles) than the aqueous KOH electrolyte (typically 7000 cycles) but the overall optical contrast remains higher with the liquid one. The use of a corrosion protection thin layer on top of the NiO–TiO₂ layer improves the cycling stability but worsens the contrast. These first results show that a gel electrolyte based on a natural product like starch but impregnated with KOH is a promising material to be used in such EC devices, especially because of its simple method of preparation and its extremely low cost.

Acknowledgements

The authors are indebted to FAPESP, CNPq, CAPES, PROBAL and the State of Saarland for their financial support.

References

- [1] C.G. Granqvist, *Handbook of Inorganic Electrochromic Materials*, Elsevier, Amsterdam, 1995.
- [2] N.A. O'Brien, J. Gordon, H. Mathew, B.P. Hichwa, *Thin Solid Films* 345 (1999) 312.
- [3] J.P. Cronin, T.J. Gudgela, S.R. Kennedy, A. Agrawal, D.R. Uhlmann, *Mater. Res.* 2 (1999) 1.
- [4] E. Avendaño, L. Berggren, G.A. Niklasson, C.G. Granqvist, A. Azens, *Thin Solid Films* 496 (2006) 30.
- [5] P.M.S. Monk, R.J. Mortimer, D.R. Rosseinsky, *Electrochromism: Fundamentals and Applications*, VCH, Weinheim, 1995.
- [6] A. Surca, B. Orel, B. Pihlar, *J. Sol-Gel Sci. Technol.* 8 (1997) 743.
- [7] S.-H. Lee, S.-K. Joo, *Sol. Energy Mater. Sol. Cells* 39 (1995) 155.
- [8] A. Azens, L.K.G. Vaivars, H. Nordborg, C.G. Granqvist, *Solid State Ion.* 113–115 (1998) 449.
- [9] R. Lechner, L.K. Thomas, *Sol. Energy Mater. Sol. Cells* 54 (1998) 139.
- [10] J. Nagai, G.D. McMeeking, Y. Saitoh, *Sol. Energy Mater. Sol. Cells* 56 (1999) 309.
- [11] A. Azens, G. Gustavsson, R. Karmhag, C.G. Granqvist, *Solid State Ion.* 165 (2003) 1.
- [12] A.L. Larsson, G.A. Niklasson, *Mater. Lett.* 58 (2004) 2517.
- [13] S. Heusing, D.-L. Sun, J. Otero-Anaya, M.A. Aegerter, *Thin Solid Films* 502 (2006) 240.
- [14] F. Deckler, S. Passerini, R. Pileggi, B. Scrosati, *Electrochrom. Acta* 37 (1992) 1033.
- [15] A. Al-Kahlout, Ph.D. Thesis, University of Saarland and Leibniz-Institut für Neue Materialien, 2006.
- [16] A. Al-Kahlout, S. Heusing, M.A. Aegerter, *J. Sol-Gel Sci. Technol.*, 2006, available on line 1 June, 2006, DOI:10.1007/s10971-006-7746-727.
- [17] P. Baudry, A.C.M. Rodrigues, M.A. Aegerter, L.O. Bulhoes, *J. Non-Cryst. Solids* 121 (1990) 319.
- [18] H. Schmidt, H. Krug, N. Merl, A. Moses, P. Judeinstein, A. Berni, *Electrochromic thin-film systems and components thereof*, Patent WO 95/28663, April 18, 1994.
- [19] R.G.F. Costa, C.O. Avellaneda, A. Pawlicka, S. Heusing, M.A. Aegerter, *Mol. Cryst. Liq. Cryst.* 447 (2006) 363.
- [20] <<http://chem.ch.huji.ac.il/~eugeniik/faq.htm>>.
- [21] A. Al-Kahlout, M.A. Aegerter, *Solar Energy Materials & Solar Cells*, submitted for publication.
- [22] W.F. Chen, S.Y. Wu, Y.F. Ferng, *Mater. Sci.* 60 (2006) 790.
- [23] P.A. Williams, A.C. Jones, J.F. Bickley, A. Steiner, H.O. Davies, T.J. Leedham, S.A. Impey, J. Garcia, S. Allen, A. Rougier, A. Blyr, *J. Mater. Chem.* 11 (2001) 2329.